González-Pedro, V.; Veldhuis, SA.; Begum, R.; Bañuls Polo, M.; Bruno, A.; Mathews, N.; Mhaisalka, S.... (06-2). Recovery of Shallow Charge-Trapping Defects in CsPbX3 Nanocrystals through Specific Binding and Encapsulation with Amino-Functionalized Silanes. ACS Energy Letters. 3(6):1409-1414. https://doi.org/10.1021/acsenergylett.8b00498

Recovery of Shallow Charge Trapping Defects in $CsPbX_3$ Nanocrystals through Specific Binding and Encapsulation with Amino-functionalized Silanes

Victoria González-Pedro[1], Sjoerd A. Veldhuis[2],* Raihana Begum[2], María José Bañuls[1], Annalisa Bruno[2], Nripan Mathews[2,3],* Subodh Mhaisalkar[2,3] and Ángel Maquieira[1]*

[1] IDM, Instituto Interuniversitario de Reconocimiento Molecular y Desarrollo Tecnológico, Departamento de Química, Universitat Politècnica de València. E-mail: vicgonpe@upvnet.upv.es

[2] Energy Research Institute at NTU (ERI@N), Nanyang Technological University, Research Techno Plaza, X-Frontier Block Level 5, Singapore 637553, Singapore. E-mail: sveldhuis@ntu.edu.sg and nripan@ntu.edu.sg

[3] School of Materials Science and Engineering, Nanyang Technological University, 50 Nanyang Avenue, Singapore 639798, Singapore

ABSTRACT. Here, we report a facile methodology to restore photoluminescence of $CsPbBr_3$ nanocrystals (NCs) based on their post-synthetic modification with 3-aminopropyltriethoxysilane (APTES). By this methodology a stark PL recovery factor of near two-fold was obtained regarding their uncoated counterparts. ^{1}H-NMR studies confirmed the presence of APTES on the NCs shell, and provided more insight into the nature of the alkoxysilane passivation mechanisms. We further highlight that, contrary to expectations, preferential attachment of APTES does not take place through their amine terminal groups. The proposed surface-repair strategy can be extended to other halide compositions, yielding similarly effective four-fold and two-fold PL enhancements for $CsPbCl_3$ and $CsPbI_3$ NCs, respectively. Our work thus exemplifies that careful management of the PS NCs interfaces and surface engineering are one of the most important frontiers in this emerging class of optoelectronic materials.

TOC graphic

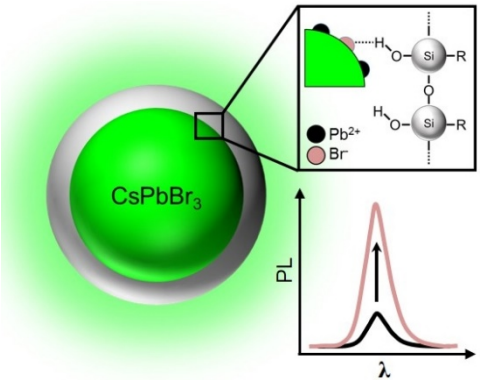

Colloidal nanocrystals (NCs) of $CsPbX_3$ metal halide perovskites (PS) are a new class of materials which have awakened great expectations in the field of multiphoton-imaging applications and optoelectronic materials due to their ultrahigh photoluminescence (PL) quantum yield (~99%),[1] size and composition tunable emission properties with a wide color gamut[2-3] and suppresion of photoluminescence intermittency[4], among other appealing features[5-7]. Nonetheless, the future of this emerging technology needs to address two main challenges to become economically viable. Firstly the stability issues at high humidity and in polar/protic solvents should be addressed, while the understanding of their surface chemistry should be expanded to fabricate processable NCs which remain structurally intact in different environment and processing conditions.

One of the most fascinating facets of lead halide perovskite materials are their unique defect physics, where charge recombination mostly occurs through the surface defects states, and recombination in the grain interior appears to be negligible. Therefore, interface engineering plays a major role in their final optical properties. Accordingly, several reports demonstrate the performance enhancement in both solar cells and LEDs through insertion of a thin insulating layer on top of the perovskite film, which acts as a blocking layer inhibiting electron recombination via shallow trap states.[8-11] Notably, due to the large surface-to-volume ratio of perovskite NCs, encapsulation strategies constitute a requisite platform to concomitantly enhance their surface passivation and optoelectronic performance. In this regard, Koscher *et al*.[1] have reported a 30% recovery of the PLQY for $CsPbBr_3$ NCs via thiocyanate interaction with undercoordinated Pb atoms on the surface. In other reports, the PLQY of $CsPbBr_3$ was improved to ~50% and ~70% by postsynthetic treatment with bromide olefin salts.[12-13] Despite the apparent benefits, currently there are only few reports on encapsulating perovskite NCs, and many of this

new class of performing-enhancing species still remain unexplored. Therefore, a better understanding of the surface chemistry and proper functionalization of such NCs - which determines their interaction with the environment - is required to prepare solution-procesable PS NCs of improved colloidal stability and water resistance properties.

Here we propose the use of amino-functionalized alkoxysilanes as passivating agent. For decades, alkoxysilanes have been extensively used as capping ligands for semiconductor quantum dots, and constitute a promising route for encapsulating PS QDs due to their well-developed and understood chemistry and facile conjugation with various functional groups (i.e. to enable further functionalization through polymerization).[14] Towards this goal, Zhang *et al*. reported PS NCs coated with sterically hindered alkoxysilanes as capping ligands, which exhibit enhanced stability in protic solvents.[15] In a reverse strategy, PS degradation in protic solvents was prevented by a silica matrix in PS/SiO_x nanocomposites prepared by embedding PS NCs in mesoporous SiO_2.[16-17] Despite the rising number of investigations employing alkoxysilane ligands, most of these studies are solely focused on addressing stability matters; i.e. without a detailed investigation of the binding mechanisms at the alkoxysilane-perovskite interface and the consequent passivation of shallow surface states.

In this letter, we demonstrated a post-synthetic modification of $CsPbBr_3$ NCs with alkoxysilanes and studied its effect on the NCs' optical properties. For this purpose, we have chosen 3-aminopropyltriethoxysilane (APTES) as a capping ligand, as it can anchor on the PS surface via hydrogen bounds with its terminal amine or ammonium group, while simultaneously allowing the silane primers to polymerize into a polymeric network surrounding the NCs' surface. A systematic and reproducible PL enhancement was observed upon APTES addition to the colloidal NC solution. Transmission electron microscopy (TEM) and proton nuclear magnetic resonance spectroscopy (^{1}H-NMR) have

enabled to identify an alkoxysilane-shell surrounding the perovskite NCs. In this framework, ^{1}H-NMR, is a widely employed technique for characterizing NC ligand shells, thus enabling us to shed a light on the possible passivation mechanisms. These findings are a first attempt to decipher the anchoring mechanisms of alkoxysilanes on the perovskite NC surface and will assist towards rational design of robust and efficient encapsulation shells based on alkoxysilane units.

$CsPbBr_3$ NCs were synthesized following the procedure described by Kovalenko *et al.*[2] (Figure S1). The synthesis yielded monodispersed cuboidal-shaped NCs with 8.7 ± 1.2 nm edge-length and PLQY~ 45%. For the alkoxysilane post-synthetic treatment, fresh perovskite NCs (2 mg mL^{-1}) were treated with increasing equivalents of APTES and stirred for 15 min (here, one equivalent corresponds to the molar amount required to form one alkoxysilane monolayer on the NC surface). Then, HBr was added and the colloidal solution was stirred for 30 min prior to further testing. The APTES and aqueous HBr were linked in an specific ratio [Si]:[OR]:[H_2O] = 1:3:3. The synthesis in absence of HBr, named PS@APTES, was also prepared as a reference. In typical sol-gel reactions, the initial reaction stage comprises the hydrolysis of the metal alkoxide precursor after reaction with water, followed by a sequence of condensation reactions (Equation 1-3). In case of Si alkoxides the reactivity is sufficiently low, such that both hydrolysis and condensation reactions follow two distinct steps. The presence of three equivalents of water (i.e. present in HBr) is thus expected to be sufficient to start and complete the hydrolysis reaction, whereas the proton of HBr is expected to act as a catalyst; resulting in the formation of a network of Si-O-Si chemical linkages around the NC surface.

$$Si(OR)_3 + 3H_2O \rightarrow Si(OH)_3 + 3R\text{-}OH \qquad \text{(Hydrolysis)} \qquad (1)$$

$$Si\text{-}OH + HO\text{-}Si \rightarrow Si\text{-}O\text{-}Si + H_2O \qquad \text{(Oxolation)} \qquad (2)$$

Si-OH + RO-Si → Si-O-Si + R-OH (Alkoxylation) (3)

The PL emission spectra are depicted in Figure 1a and Figure S2 and the evolution of PLQY for different amounts of alkoxysilane are summarized in Figure 1b. A stark PL enhancement was observed after APTES addition. Sample treated with 11.5 eq. of APTES, displayed a record increase of PL emission, showing a near two-fold increase over the bare PS NCs. Remarkably, a large excess of organosilane (≥ 46 eq.), led to rapid chemical decomposition of the perovskite, and therefore a drastic drop in PL emission was observed. Thin nanocrystal films prepared on glass substrates (Figure S3), displayed similar enhancements after modification than samples measured in solution. Samples modified with both APTES and HBr (PLQY ~73%) exhibited ~1.7 times higher emission yields than untreated (washed) $CsPbBr_3$ NC films.

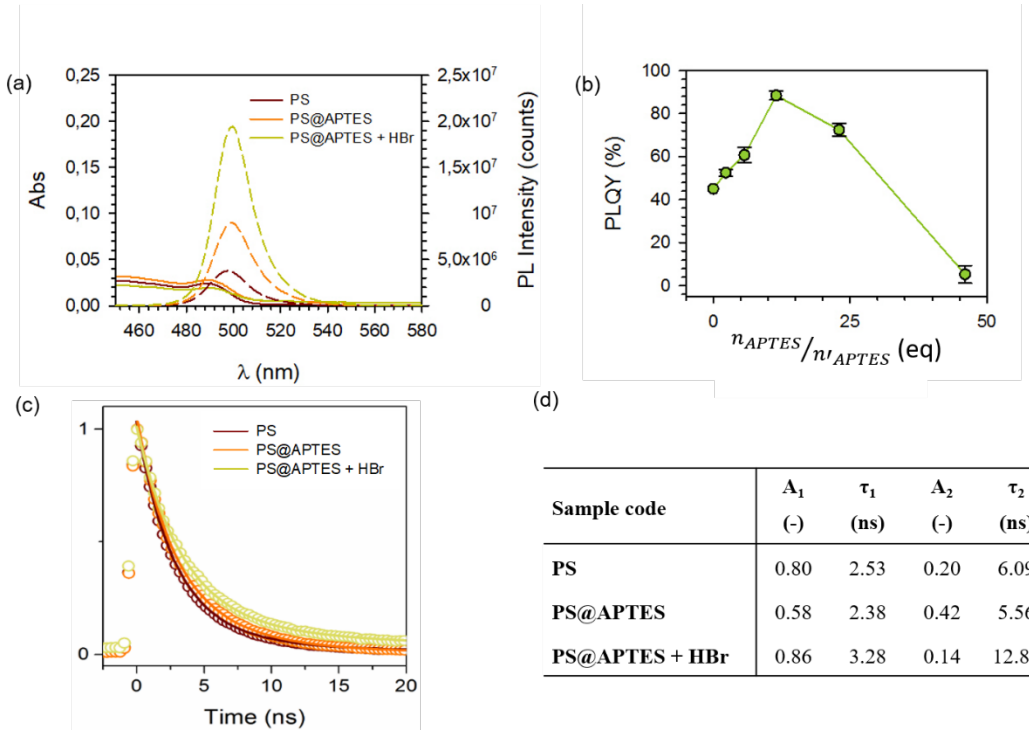

Sample code	A_1 (-)	τ_1 (ns)	A_2 (-)	τ_2 (ns)	τ_{ave} (ns)
PS	0.80	2.53	0.20	6.09	3.26
PS@APTES	0.58	2.38	0.42	5.56	3.56
PS@APTES + HBr	0.86	3.28	0.14	12.81	4.60

Figure 1. (a) Absorbance (solid line) and photoluminescence spectra (dashed line) of bare $CsPbBr_3$ NCs (brown line), treated with 11.5 eq. of APTES plus HBr (green line) and treated with alkoxysilane in the absence of acidic catalyst (orange line). PL spectra were

recorded using an excitation wavelength of λ_{exc}= 400 nm. (b) Evolution of emission yield after APTES addition. (c) Time-resolved PL spectra and (d) table displaying PL lifetimes of $CsPbBr_3$ NCs shown in (a). The PL decay curves are fitted using a biexponential decay function, where A and τ refer to the decay amplitudes and PL lifetimes, respectively. The average lifetime (τ_{ave}) is calculated as: $\tau_{ave} = A_1 \cdot \tau_1 + A_2 \cdot \tau_2$.

The origin of this striking PL enhancement may arise from the effective surface passivation by the APTES ligands, whereby non-radiative surface defects are reduced through binding to the perovskite surface. The defect passivation may take place via: (*i*) the formation of dative-covalent bonds between amines of the silane network and under-coordinated Pb^{2+} sites;[10] (*ii*) hydrogen bond formation between remaining silanols and surface bromide sites;[9, 18] or (*iii*) the formation of hydrogen bonds through protonated amines and bromide dangling bonds.[19] Our photoluminescence data is in good agreement with previous reported data, where blocked surface recombination and enhanced photoconversion efficiencies of solar cells were demonstrated for silane layers on top of perovskite films.[8-9, 11] Time-resolved photoluminescence measurements also show an enhancement of the PL lifetime upon APTES treatment (see Figure 1 c and d). Notably, the references PS and PS@APTES sample prepared in absence of HBr renders a much lower PL emission enhancement compared to samples treated with a combination of APTES and HBr. This corroborates well with the increased average PL lifetime (increase from ca. 6 to 12.8 ns), longer radiative lifetime and larger contribution of the radiative component for these samples. This behavior may arise from enhanced passivation of the $CsPbBr_3$ NCs triggered by growth/nucleation of ordered silica islands surrounding the NCs surfaces. In order to rule out that PL boosting effect arises merely from Br^- ions enrichment in the NCs environment, as reported in literature [20-22], control experiments of PS treated only with aqueous HBr (i.e. in the absence of alkoxysilane) were carried out

(Figure S4, SI). Here, only a small enhancement in emission yields is observed for control samples treated with HBr; presumably because of the passivation of undercoordinated Pb^{2+} vacancies by Br^- ions. Despite the minor contribution of Br^- to the surface passivation and PL emission, the control experiments clearly unveil that APTES dominates in the effective passivation of $CsPbBr_3$ NCs' defect states.

Transmission electron microscopy (TEM) and ^{1}H-NMR were performed to better understand the nature of the alkoxysilane shell. Both treated and untreated NCs exhibited uniform size distributions and regular cuboid-shaped morphologies with average NC sizes of 8.3 ± 1.3 nm and 8.7 ± 1.7 nm, respectively (Figure 2). As shown, the APTES treatment did not induce any structural changes to the NCs composite. The fingerprint of an alkoxysilane network can be seen in only a small population of NCs (~10-15%) for the NCs treated with larger amount of silane (23 eq), observed as a 1-2 nm-thick uniform shell surrounding the NC. To verify the presence of the APTES on samples treated with 11.5 eq., the spatial distribution and elemental ratios were analyzed by energy-dispersive X-ray spectroscopy elemental mapping (EDX; Figure S5). The EDX spectrum shows a uniformly distributed elemental signal of Si, O, C and N elements which corroborates well with the presence of the silane capping ligand.

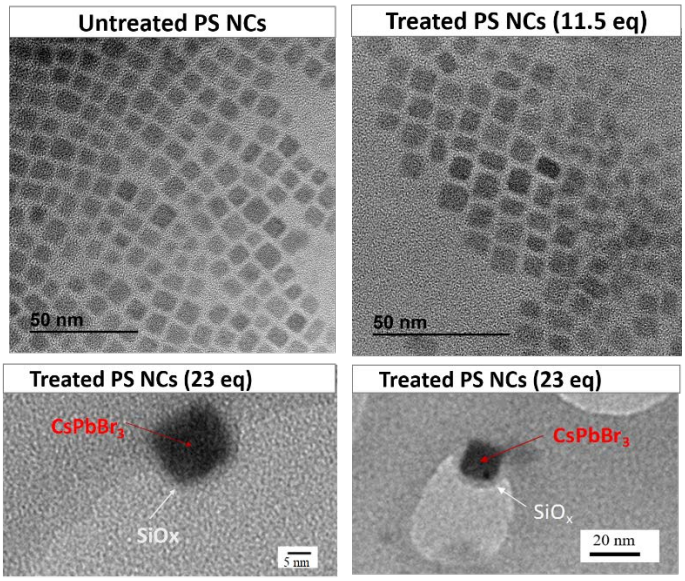

Figure 2. Transmission electron microscopy images for cuboidal-shaped PS@APTES + HBr core-shell NCs.

The composition of the shell material was further analyzed by means of ^{1}H-NMR to confirm the presence of the alkoxysilane capping ligands on the NC surface. For this purpose, PS NCs were washed three times in hexane, dried for 24 h under vacuum, and finally redispersed in $CDCl_3$ for spectroscopic analysis. Figure 3 depicts the proton spectrum of bare perovskite NCs (pink), PS@APTES + HBr (green), and the 3-(aminopropyl)triethoxysilane. Reference spectra of oleic acid and oleylamine are provided in the Supporting Information (Figure S6). The perovskite NC spectrum shows the presence of characteristic resonance peaks of both oleic acid and oleylamine, confirming the presence of both capping ligands in the sample.[19, 23] By employing an internal standard for quantification, tetramethylsilane (TMS), from the integrated peak areas of the olefin alkene resonances (A7, A8, B7, and B8), we calculated a total concentration oleyl species of 3.44 mM. It is noteworthy to mention that both olefin α-methylene groups, A16 and B16, feature a broaden and less sharp peak, which can be ascribed to the bound ligand effect.

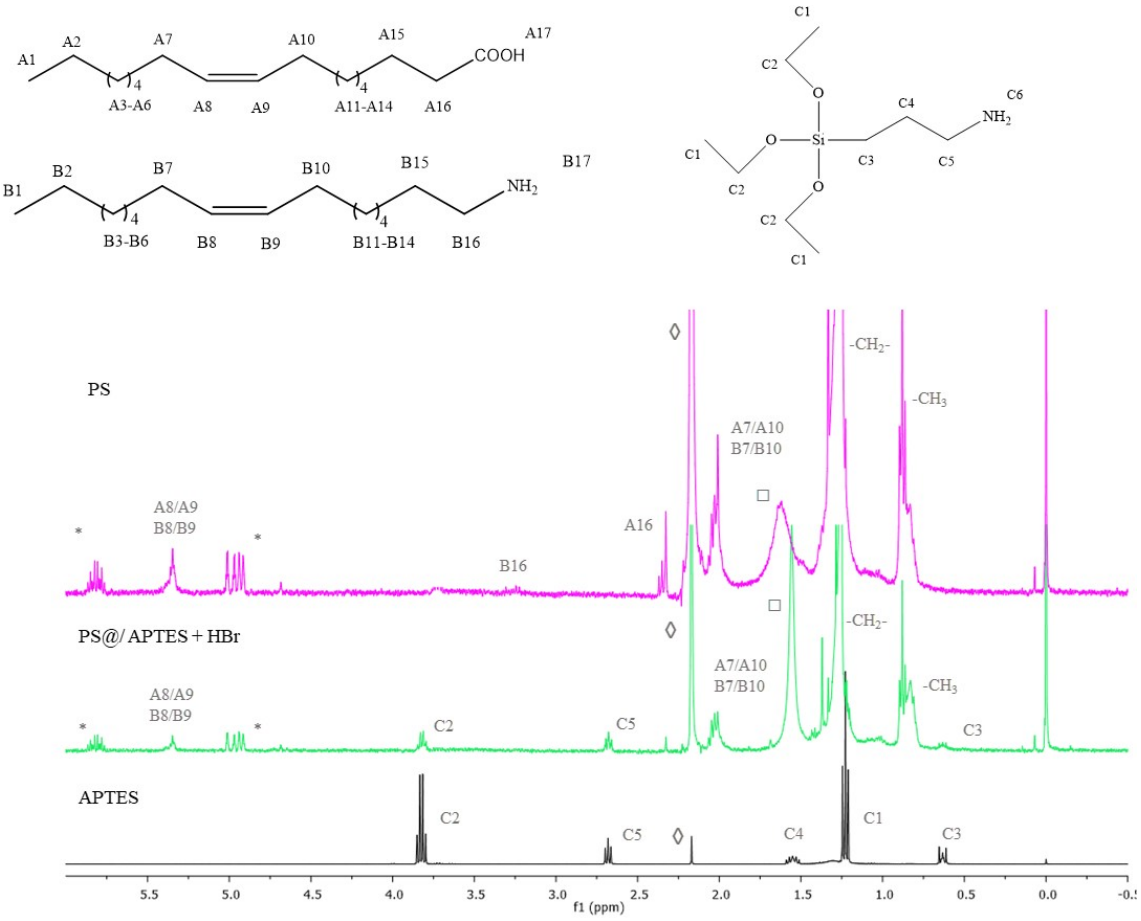

Figure 3. ^{1}H-NMR spectra ($CDCl_3$, 500 MHz) of bare $CsPbBr_3$ NCs (pink), treated with 11.5 eq. of APTES plus HBr (green) and reference standard of APTES. Concentration of NCs are 1.4 and 1 µM for bare and treated NCs, respectively. The chemical structures of the different capping ligands are depicted on the top. The proton assignment is denoted in the spectra. (*) The characteristic resonances of 1-octadecene (ODE) at δ = 4.94 and 5.8 ppm indicate the small presence of solvent retained after washing, which can be attributed to the ODE intercalation on the oleyl-based shell. (□) A pool of labile hydrogens at δ = 1.5-1.8 ppm is also present in the ^{1}H-NMR spectrum, possibly due to a minor contamination with water. (◊) All samples present a peak at δ = 2.17 ppm which is ascribed to an impurity of the $CDCl_3$.

It can be seen that the PS@APTES + HBr spectrum exhibits the characteristic quadruplet of the APTES methylene belonging to the ethoxy moiety (C2) at δ = 3.83 ppm, the triplet of the amine α-methylene (C5) at δ = 2.68 ppm. Similarly, the methylene group in close proximity of silicon (C3) δ = 0.63 ppm, as well as the characteristic resonance peaks of oleyl species are present (although in this spectrum α- methylene group for carboxylic and amine olefins cannot be observed, it is noteworthy to remark that protons close to the surface frequently remain undetected[24]). From the peak integration of the alkene resonances, C3 and C5 (displayed in Figure S7), we estimated a ligand concentration of 1.2 mM and 0.72 mM for silane and oleyl species, respectively. Our data highlights that the alkoxysilane partly exchanged the original oleyl ligands, and thus plays an active role in the $CsPbBr_3$ NCs surface passivation mechanism.

In order to gain further insights into the silane surface passivation mechanism, PS NCs were treated with trimethoxypropylsilane (TMPS); Figure S8a, and an alkylamine of different chain length plus HBr (Figure S9) as control experiments. The PS NCs treated with TMPS displayed a 44% PL increase (PLQY~69%), while in the case of alkylamines only a slight PL increase was observed (i.e. much lower than APTES and TMPS); presumably due to the ammonium linkage with surface bromides via hydrogen bound formation. In light of our findings, we hypothesize that, contrary to expectations, the alkoxysilane anchors preferentially on NCs surface through its remaining silanol groups (it is remarkably that silanol protons often remain undetected by ^{1}H-NMR spectroscopy because of the hydrogen bond formation). Our proposed hypothesis was further confirmed by ^{1}H-NMR spectroscopy. The PS@TMPS + HBr spectrum displayed in Figure S8b exhibit the characteristic resonances of TMPS at δ = 3.53, 1.45, 0.97, and 0.66 ppm and peak integration revealed a silane and olefin concentration of 14.13 mM and 0.463 mM, respectively, revealing that TMPS almost completely displaced all the original

oleyl-based shell. The larger ratio of silane species on the NC surface could therefore be attributed to the faster hydrolysis-condensation kinetics of methoxy-based silanes, compared to their ethoxy counterparts; resulting in more a rapid encapsulation. Despite the smaller PL recovery for the TMPS treatment compared to APTES, our experiments unambiguously uncovered the active role of free dangling silanol-groups in the perovskite surface passivation mechanism, as reported in previous studies for NCs thin films.[9, 18] A schematic diagram of the proposed silane passivation mechanism is illustrated in Figure 4.

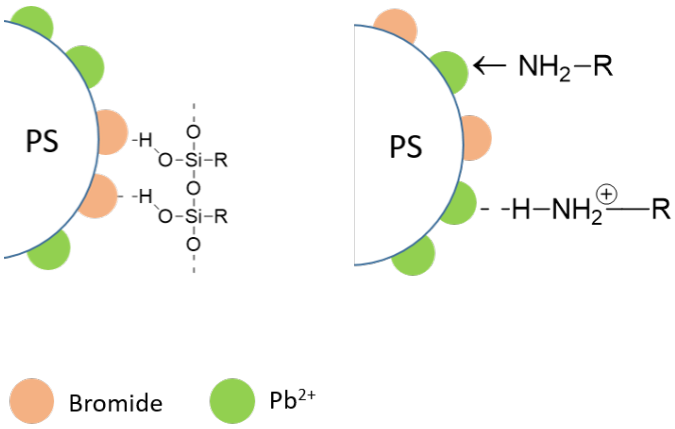

Figure 4. Schematic diagram showing the proposed alkoxysilane ligand-perovskite binding motif.

In order to inspect the versatility of our method we have extended the APTES surface treatment to other halide compositions; where $CsPbCl_3$ and $CsPbI_3$ were synthesized according to previously reported procedures.[2] In order to circumvent further halide exchange during the surface treatment, HCl and HI were added to APTES – instead of HBr – for $CsPbCl_3$ and $CsPbI_3$, respectively. The absorption and PL spectra of the different halide compositions are depicted in Figure 5. We note that the PL/absorbance spectra of $CsPbI_3$ after treatment with APTES/HI is missing, due to the cubic-to-orthorhombic transformation to the inactive yellow δ-$CsPbI_3$ phase. We infer that this

transformation was accelerated by the aqueous acidic catalyst, which completely quenched the photoluminescence. Despite the latter, our methodology was successfully extended to all halide compositions, which exhibited a stark PL increase upon addition of APTES and APTES+HX. This effect was strongest for $CsPbCl_3$ NCs, with a striking four-fold PL enhancement after treatment with APTES and HCl, compared to a two-fold enhancement observed for both the Br and I analogues.

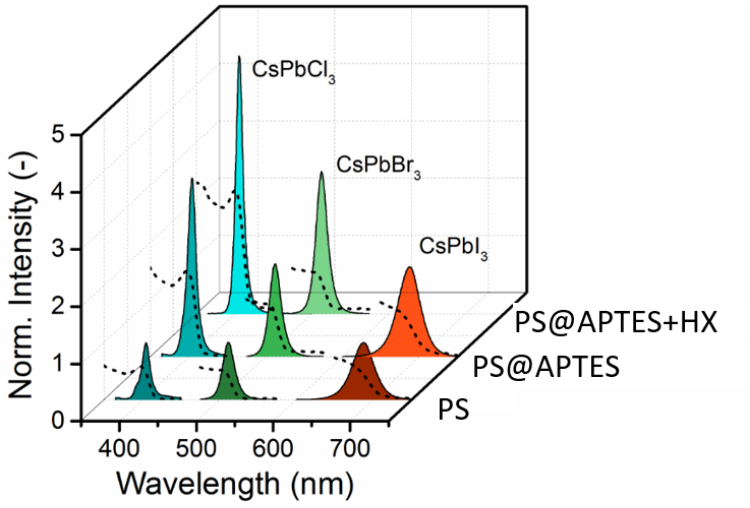

Figure 5. Normalized absorbance (dashed lines) and photoluminescence spectra of $CsPbX_3$ (X = Cl, Br, or I) NCs after BuOH washing, APTES treatment (11.5 eq.), and APTES+HX treatment (whereby the halogen in the acidic aqueous solution matches the halides of the respective perovskite). PL spectra were recorded using an excitation wavelength of λ_{exc}= 350 nm and 400 nm for of $CsPbCl_3$/$CsPbBr_3$ and $CsPbI_3$ NCs, respectively. Note: upon addition of HI to the $CsPbI_3$ NCs + APTES mixture, the $CsPbI_3$ transformed to the inactive orthorhombic (yellow) δ-$CsPbI_3$ phase.

In summary, we have presented a new strategy to enhance the photoluminescence efficiency of $CsPbX_3$ NCs based on the post-synthetic treatment with amine-terminated alkoxysilanes (i.e. 3-aminopropyltriethoxysilane; APTES), which is applicable to all

halide analogues. Compared to their untreated counterparts, near two-fold emission efficiency improvements were recorded for $CsPbBr_3$ and $CsPbI_3$, while for $CsPbCl_3$ NCs the surface-repair method displayed a near four-fold enhancement. ^{1}H-NMR analysis further elucidated the nature of the shell composition and the underlying SiO_x coverage mechanism. Contrary to expectations, our findings highlight that preferential attachment of APTES takes place through hydrogen bond formation between silanol groups and bromide dangling bonds, and not via their terminal amine groups. The important role the silanols play in the passivation of perovskite surface defects, open new avenues towards rational design of carefully managed interfaces and robust encapsulation shells.

Acknowledgements

This work was financially supported by FEDER projects BiHolog-CTQ2016-75749-R from MINECO and GVA PROMETEO II 2014/40. V.G-P. thanks Universitat Politècnica de València for her post-doctoral fellowship (Grant-PAID-10-14) and for her research mobility grant (UPV- Research mobility grant-PAID-00-15). S.A.V., N.M. and S.M. acknowledge the financial support by the National Research Foundation, Singapore under its Competitive Research Programme (NRF-CRP14-2014-03). S.A.V. thanks Alasdair Brown for help with the nanocrystal syntheses.

Supporting Information Available: Detailed experimental methods; characterization of as-prepared nanocrystals; additional photoluminescence spectra, EDS mapping images and ^{1}H NMR analysis.

References

(1) Koscher, B. A.; Swabeck, J. K.; Bronstein, N. D.; Alivisatos, A. P. Essentially Trap-Free $CsPbBr_3$ Colloidal Nanocrystals by Postsynthetic Thiocyanate Surface Treatment. *J. Am. Chem. Soc.* **2017,** *139* , 6566-6569.

(2) Protesescu, L.; Yakunin, S.; Bodnarchuk, M. I.; Krieg, F.; Caputo, R.; Hendon, C. H.; Yang, R. X.; Walsh, A.; Kovalenko, M. V. Nanocrystals of Cesium Lead Halide Perovskites ($CsPbX_3$, X = Cl, Br, and I): Novel Optoelectronic Materials Showing Bright Emission with Wide Color Gamut. *Nano Lett.* 2015, 15, 3692-3696.

(3) Nedelcu, G.; Protesescu, L.; Yakunin, S.; Bodnarchuk, M. I.; Grotevent, M. J.; Kovalenko, M. V. Fast Anion-Exchange in Highly Luminescent Nanocrystals of Cesium Lead Halide Perovskites ($CsPbX_3$, X = Cl, Br, I). *Nano Lett.* **2015**, 15, 5635-5640.

(4) Swarnkar, A.; Chulliyil, R.; Ravi, V. K.; Irfanullah, M.; Chowdhury, A.; Nag, A. Colloidal $CsPbBr_3$ Perovskite Nanocrystals: Luminescence beyond Traditional Quantum Dots. *Angew. Chem. Int. Ed. 2015*, 54, 15424-15428.

(5) Sutherland, B. R.; Sargent, E. H., Perovskite Photonic Sources. *Nat. Photonics* **2016**, 10, 295-302.

(6) Amgar, D.; Stern, A.; Rotem, D.; Porath, D.; Etgar, L. Tunable Length and Optical Properties of $CsPbX_3$ (X = Cl, Br, I) Nanowires with a Few Unit Cells. *Nano Lett*. **2017**, 17, 1007-1013.

(7) Veldhuis, S. A.; Boix, P. P.; Yantara, N.; Li, M.; Sum, T. C.; Mathews, N.; Mhaisalkar, S. G. Perovskite Materials for Light-Emitting Diodes and Lasers. *Adv. Mater*. **2016**, 28, 6804-6834.

(8) Wang, Q.; Dong, Q.; Li, T.; Gruverman, A.; Huang, J. Thin Insulating Tunneling Contacts for Efficient and Water-Resistant Perovskite Solar Cells. *Adv. Mater.* **2016**, 28, 6734-6739.

(9) Zhang, J.; Hu, Z.; Huang, L.; Yue, G.; Liu, J.; Lu, X.; Hu, Z.; Shang, M.; Han, L.; Zhu, Y. Bifunctional Alkyl Chain Barriers for Efficient Perovskite Solar Cells. *Chem. Comm.* **2015**, 51, 7047-7050.

(10) Wen, X.; Wu, J.; Gao, D.; Lin, C. Interfacial Engineering with Amino-functionalized Graphene for Efficient Perovskite Solar Cells. *J. Mater. Chem. A* **2016**, 4, 13482-13487.

(11) Yun, J. H.; Lee, I.; Kim, T.-S.; Ko, M. J.; Kim, J. Y.; Son, H. J. Synergistic Enhancement and Mechanism Study of Mechanical and Moisture Stability of Perovskite Solar Cells Introducing Polyethylene-imine into the $CH_3NH_3PbI_3$/HTM Interface. *J. Mater. Chem. A* **2015**, 3, 22176-22182.

(12) .Zhang, D.; Yu, Y.; Bekenstein, Y.; Wong, A. B.; Alivisatos, A. P.; Yang, P. Ultrathin Colloidal Cesium Lead Halide Perovskite Nanowires. *J. Am. Chem. Soc.* **2016**, 138, 13155-13158.

(13) Pan, J.; Quan, L. N.; Zhao, Y.; Peng, W.; Murali, B.; Sarmah, S. P.; Yuan, M.; Sinatra, L.; Alyami, N. M.; Liu, J.; *et al.* Highly Efficient Perovskite-Quantum-Dot Light-Emitting Diodes by Surface Engineering. *Adv. Mater.* **2016**, 28, 8718-8725.

(14) Nann, T.; Mulvaney, P., Single Quantum Dots in Spherical Silica Particles. *Angew. Chem. Int. Ed.* **2004**, 43, 5393-5396.

(15) Luo, B.; Pu, Y.-C.; Lindley, S. A.; Yang, Y.; Lu, L.; Li, Y.; Li, X.; Zhang, J. Z. Organolead Halide Perovskite Nanocrystals: Branched Capping Ligands Control Crystal Size and Stability. *Angew. Chem. Int. Ed.* **2016**, 55, 8864-8868.

(16) Huang, S.; Li, Z.; Kong, L.; Zhu, N.; Shan, A.; Li, L. Enhancing the Stability of $CH_3NH_3PbBr_3$ Quantum Dots by Embedding in Silica Spheres Derived from Tetramethyl Orthosilicate in "Waterless" Toluene. *J. Am. Chem. Soc.* 2016, 138, 5749-5752.

(17) Wang, H.-C.; Lin, S.-Y.; Tang, A.-C.; Singh, B. P.; Tong, H.-C.; Chen, C.-Y.; Lee, Y.-C.; Tsai, T.-L.; Liu, R.-S. Mesoporous Silica Particles Integrated with All-Inorganic CsPbBr3 Perovskite Quantum-Dot Nanocomposites (MP-PQDs) with High Stability and Wide Color Gamut Used for Backlight Display. *Angew. Chem. Int. Ed.* **2016**, 55, 7924-7929.

(18) Li, X.; Ibrahim Dar, M.; Yi, C.; Luo, J.; Tschumis, M.; Zakeeruddin, S. M.; Nazeeruddin, M. K.; Han, H.; Grätzel, M. Improved Performance and Stability of Perovskite Solar Cells by Crystal Crosslinking with Alkylphosphonic Acid ω-ammonium Chlorides. *Nat Chem.* **2015**, 7, 703-711.

(19) Pan, A.; He, B.; Fan, X.; Liu, Z.; Urban, J. J.; Alivisatos, A. P.; He, L.; Liu, Y. Insight into the Ligand-Mediated Synthesis of Colloidal $CsPbBr_3$ Perovskite Nanocrystals: The Role of Organic Acid, Base, and Cesium Precursors. *ACS Nano* **2016**, 10, 7943-7954.

(20) Li, X.; Wu, Y.; Zhang, S.; Cai, B.; Gu, Y.; Song, J.; Zeng, H. $CsPbX_3$ Quantum Dots for Lighting and Displays: Room-Temperature Synthesis, Photoluminescence Superiorities, Underlying Origins and White Light-Emitting Diodes. *Adv. Funct. Mater.* **2016**, 26, 2435-2445.

(21) Woo, J. Y.; Kim, Y.; Bae, J.; Kim, T. G.; Kim, J. W.; Lee, D. C.; Jeong, S. Highly Stable Cesium Lead Halide Perovskite Nanocrystals through in Situ Lead Halide Inorganic Passivation. *Chem. Mater.* **2017**, 29, 7088-7092.

(22) Kang, J.; Wang, L.-W. High Defect Tolerance in Lead Halide Perovskite $CsPbBr_3$. *J. Phys. Chem. Lett.* **2017**, 8, 489-493.

(23) De Roo, J.; Ibáñez, M.; Geiregat, P.; Nedelcu, G.; Walravens, W.; Maes, J.; Martins, J. C.; Van Driessche, I.; Kovalenko, M. V.; Hens, Z. Highly Dynamic Ligand Binding and Light Absorption Coefficient of Cesium Lead Bromide Perovskite Nanocrystals. *ACS Nano* **2016**, 10, 2071-2081.

(24) Boles, M. A.; Ling, D.; Hyeon, T.; Talapin, D. V. The Surface Science of Nanocrystals. *Nat. Mater.* **2016**, 15, 141.